

Evidence for the Influence of Surface Heat Fluxes on Turbulent Mixing of Microplastic Marine Debris

TOBIAS KUKULKA

University of Delaware, Newark, Delaware

KARA L. LAW

Sea Education Association, Woods Hole, Massachusetts

GIORA PROSKUROWSKI

University of Washington, Seattle, Washington

(Manuscript received 6 December 2015, in final form 12 January 2016)

ABSTRACT

Buoyant microplastic marine debris (MPMD) is a pollutant in the ocean surface boundary layer (OSBL) that is submerged by wave-driven turbulent transport processes. This study analyzes observed MPMD surface concentrations in the Atlantic and Pacific Oceans to reveal a significant increase in concentrations during surface heating and a decrease during surface cooling. Turbulence-resolving large-eddy simulations of the OSBL for an idealized diurnal heating cycle suggest that turbulent downward fluxes of buoyant tracers are enhanced at night, facilitating deep submergence of plastics, and suppressed in heating conditions, resulting in surface-trapped MPMD. Simulations agree better with observations if enhanced mixing due to wave-driven Langmuir turbulence (LT) is included. The simulated time-dependent OSBL response results in hysteresis effects so that surface concentrations depend also on the phase of the diurnal heating cycle. The results demonstrate the controlling influence of surface heat fluxes and LT on turbulent transport in the OSBL and on vertical distributions of buoyant marine particles.

1. Introduction

Ocean surface boundary layer (OSBL) turbulence transports buoyant tracers that control a wide range of physical, biogeochemical, and environmental processes, such as those related to plankton dynamics (Denman and Gargett 1995), bubble-mediated air–sea gas transfer (Thorpe 1982; Liang et al. 2011; Gemmrich 2012), and the dispersion of pollutants (D’Asaro 2000; Kukulka et al. 2012; Yang et al. 2014; Brunner et al. 2015). Strong daytime surface heating of the OSBL results in diurnal warm layers (Price et al. 1986; Weller and Price 1988; Large et al. 1994; Li et al. 1995; Soloviev and Lukas 1997; Plueddemann and Weller 1999) that are characterized by relatively strong near-surface stratification and

turbulence suppression (Li and Garrett 1995; Min and Noh 2004; Noh et al. 2009; Kukulka et al. 2013). Sea surface cooling, on the other hand, drives ocean convection and enhances OSBL mixing (Li et al. 2005; Belcher et al. 2012). This study investigates the controlling influence of sea surface heat fluxes in conjunction with wave-driven Langmuir turbulence (LT) on near-surface distributions of buoyant microplastic marine debris (MPMD).

MPMD is widely distributed in vast regions of the subtropical gyres (Law et al. 2010, 2014; Cozar et al. 2014; Eriksen et al. 2014) and has emerged as an open-ocean pollutant (Andrady 2011; Gold et al. 2013). Previous observations and model results indicate that MPMD is vertically distributed within the upper water column due to wind- and wave-driven mixing (Kukulka et al. 2012; Kukulka and Brunner 2015; Brunner et al. 2015). In this study we exploit MPMD as a physical tracer to investigate turbulence dynamics of the OSBL subject to varying surface heat fluxes.

Corresponding author address: Tobias Kukulka, 211 Robinson Hall, School of Marine Science Policy, College of Earth, Ocean, and Environment, University of Delaware, Newark, DE 19716.
E-mail: kukulka@udel.edu

LT is a turbulent process due to the interactions of Eulerian surface currents with surface gravity waves that result in wind-aligned roll vortices (Thorpe 2004; Sullivan and McWilliams 2010; D'Asaro 2014). These Langmuir cells are characterized by relatively large turbulent length scales (Smith 1992; Plueddemann et al. 1996; Smith 1998; Gargett et al. 2004; Li et al. 2005; Tejada-Martinez and Grosch 2007; Polton and Belcher 2007; Grant and Belcher 2009) and facilitate the deep submergence of buoyant tracers throughout the OSBL (Colbo and Li 1999; Skillingstad 2003; Harcourt and D'Asaro 2010; Liang et al. 2011; Kukulka and Brunner 2015). Since buoyant tracers can be deeply submerged by LT and since surface heating weakens LT (Li and Garrett 1995; Min and Noh 2004; Noh et al. 2009; Kukulka et al. 2013), we hypothesize that surface heating substantially influences the vertical distributions of buoyant marine tracers. If the sea surface is sufficiently cooled by the atmosphere, convective turbulence enhances turbulence and may compete with wave-driven LT (Li et al. 2005; Belcher et al. 2012), which is expected to contribute further to deep mixing of buoyant tracers (Wyngaard 2010). Based on the analysis of observations and simulations of buoyant MPMD, this paper addresses the hypothesis that surface heat fluxes exert a measurable influence on turbulent OSBL transport and the near-surface distributions of buoyant marine tracers.

2. Methods

a. Observations and surface flux estimates

We analyze surface measurements from the Sea Education Association (SEA; Law et al. 2010, 2014), as described in Brunner et al. (2015). Surface MPMD has been measured from ships over several decades in the Atlantic and Pacific Oceans based on surface plankton (neuston) net tows. The net extends vertically from the surface to approximately 0.25-m depth and has a 335- μm mesh size. Plastics concentrations are determined for each tow from the number of collected plastic pieces and the corresponding tow area (1-m net width times distance towed). We analyze a subset of 708 plastic concentrations observed in the North Atlantic Ocean (between 22° and 38° N and 40° and 77° W from 2003 to 2010; Law et al. 2010) and in the North Pacific Ocean (between 19° and 41° N and 118° and 177° W from 2002 to 2012; Law et al. 2014). For each surface tow, wind speed measured by a shipboard anemometer was averaged over the duration of the tow and corrected to the wind speed at 10-m height U_{10} , assuming a logarithmic profile.

Bulk surface fluxes were determined from measured U_{10} and reanalysis data products. The mean U_{10} was

$U_{10} = 6 \text{ m s}^{-1}$ with a standard deviation of 2 m s^{-1} , and observed winds peaked at $U_{10} = 14 \text{ m s}^{-1}$. Surface momentum flux τ is parameterized with the drag coefficient from Large and Pond (1981). Net surface heat fluxes are estimated from the NCEP–NCAR Reanalysis-1 surface flux product (Kalnay et al. 1996).

Preliminary laboratory experiments on archived North Atlantic plastic samples in still water indicate that the buoyant rise speed of plastic pieces w_b varies between 0.5 and 3.5 cm s^{-1} with $w_b = 1.4 \pm 0.7 \text{ cm s}^{-1}$ (mean \pm standard deviation) for flat-shaped fragments, representing the most abundant form of plastic marine debris (Kukulka et al. 2012). For our model studies we investigate two w_b : the mean $w_b = 1.4 \text{ cm s}^{-1}$ and a lower limit $w_b = 0.7 \text{ cm s}^{-1}$, which is close to the median value found by Reisser et al. (2015).

b. Large-eddy simulations

The large-eddy simulation (LES) model set up to investigate a diurnal heating event closely follows our previous approach (Kukulka et al. 2013) with modifications to capture wave age-dependent equilibrium seas, breaking waves, and passive buoyant scalars (Kukulka and Brunner 2015). LT is modeled with the Craik–Leibovich vortex force, which is the cross product of Stokes drift and vorticity vectors (Skillingstad and Denbo 1995; McWilliams et al. 1997). Without LT, the Craik–Leibovich vortex force is zero. The numerical domain and grid is identical to the tested one from Kukulka et al. (2013) with a horizontal domain size of $160 \text{ m} \times 160 \text{ m}$ with 320×320 points and a depth of 60 m with 200 vertical points. Unlike in the study of Kukulka et al. (2013), the Coriolis parameter is $f = 10^{-4} \text{ s}^{-1}$. The initial mixed layer depth is set to 30 m, which is consistent with a limited number of temperature and salinity profile observations. Consistent with the observed mean wind speed, the wind stress is constant at $\tau = 0.054 \text{ N m}^{-2}$ [$U_{10} = 6 \text{ m s}^{-1}$ and $u_* = (\tau/\rho)^{1/2} \approx 0.7 \text{ cm s}^{-1}$, where u_* is the waterside friction velocity and ρ is the density of water], and the net surface heat flux I_0 varies diurnally as in the study by Kukulka et al. (2013). First, nighttime cooling is imposed as a surface heat flux at $t = 0 \text{ h}$ with $I_0 = -200 \text{ W m}^{-2}$. Then, I_0 continuously increases so that heating ($I_0 > 0$) associated with daytime solar insolation begins at $t = 4 \text{ h}$ and peaks at $t = 8 \text{ h}$ with $I_0 = 500 \text{ W m}^{-2}$. After $t = 8 \text{ h}$, I_0 continuously decreases and the ocean surface cools again for $t > 12 \text{ h}$. For heating conditions, I_0 is specified as incoming shortwave radiation by an exponentially decaying heat source following the model by Paulson and Simpson (1977) for clear ocean water. The imposed range of heat fluxes covers 90% of the surface heat fluxes during the observation period. The wave field is prescribed based on an

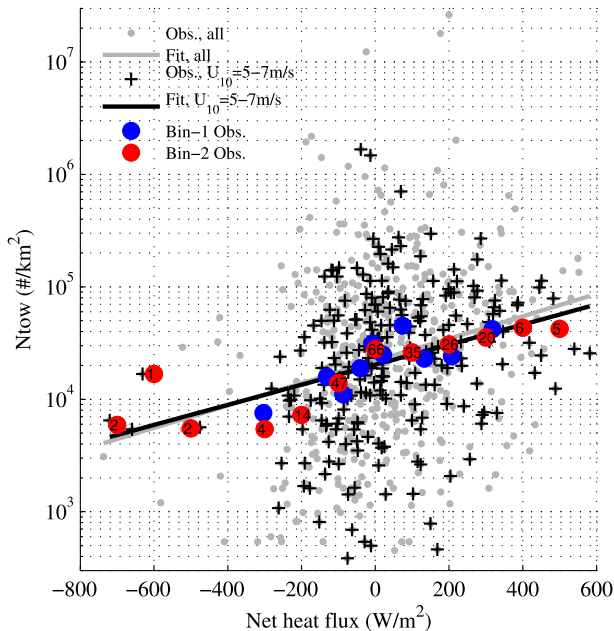


FIG. 1. Surface MPMD concentrations N_{tow} vs net surface heat flux, all observations (gray dots), subsampled observations (black pluses) for $5 < U_{10} < 7 \text{ m s}^{-1}$, and corresponding linear regression fit lines based on the empirical model [(1)]. The regression slope is $m = (2.3 \pm 0.7) \times 10^{-3}$ for all observations and $m = (2.1 \pm 1.0) \times 10^{-3}$ for observations with $5 < U_{10} < 7 \text{ m s}^{-1}$. The colored dots show observations for $5 < U_{10} < 7 \text{ m s}^{-1}$ averaged into bins with 1) equal number of points (10% of total number of points) (blue) and 2) fixed bin width with 100 W m^{-2} intervals (red, number of points in each bin shown). The regression slope is $m = (2.5 \pm 1.5) \times 10^{-3}$ for the first binning and $m = (2.2 \pm 1.1) \times 10^{-3}$ for the second binning option (regression lines not shown).

empirical wave height spectrum for a fully developed sea with a significant wave height $H_s = 0.9 \text{ m}$ (Kukulka and Brunner 2015; Brunner et al. 2015). The resulting turbulent Langmuir number $\text{La}_t = \sqrt{u_*}/u_s = 0.3$ is characteristically low, representative of wave-driven ocean LT (McWilliams et al. 1997; Li et al. 2005; here u_s is the surface Stokes drift).

3. Evidence for heat flux effects

a. Observations

To provide intuitive observational evidence for the effects of net surface heat flux I_0 on measured MPMD surface concentrations N_{tow} , we first directly relate N_{tow} to I_0 (gray dots, Fig. 1). Despite substantial scatter due to spatial variability and varying wind and wave forcing, smaller N_{tow} values are found for stronger sea surface cooling, whereas greater N_{tow} estimates occur for stronger sea surface heating. This suggests that convective cooling increases turbulence and enhances the deep submergence of plastic pieces. Surface heating, on the

other hand, appears to suppress turbulent mixing so that plastic pieces are more surface trapped and near-surface concentrations are enhanced. During the observation period, U_{10} and I_0 are only weakly correlated with a correlation coefficient of -0.15 so that the observed dependence of N_{tow} on I_0 is not an artifact due to correlated U_{10} and I_0 . A linear regression analysis based on the empirical model

$$\log(N_{\text{tow}}) = mI_0 + a \quad (1)$$

yields a slope $m = (2.3 \pm 0.7) \times 10^{-3}$ (gray line), which indicates that higher surface concentrations are associated with greater surface heating (the number following the \pm symbol denotes the 95% confidence interval, and I_0 and N_{tow} are nondimensionalized by their respective units for the regression analysis). Note that the confidence interval provides a straightforward measure of uncertainty based on standard statistical analyses. However, uncertainties in the distributions of N_{tow} , w_b , and I_0 would need to be taken into account for a more rigorous analysis of confidence intervals, which is beyond the scope of this note.

For a given I_0 , the effects of heating on N_{tow} depend on wind speed and sea state. For sufficiently strong wind- and wave-driven turbulence, the influence of surface heating or cooling is insignificant (Li et al. 2005; Belcher et al. 2012). For weak winds and small waves, surface heating effects on N_{tow} are also negligible because heating only further suppresses already weak turbulence. Surface cooling, on the other hand, drives turbulence dominantly due to convection in conditions with weak winds and small waves. Thus, variable winds and waves cause a nonunique relationship between N_{tow} and I_0 and contribute to the observed scatter in Fig. 1.

To assess more systematically the influence of surface heating on plastic distributions, we consider a narrow U_{10} range between 5 and 7 m s^{-1} , centered around the mean U_{10} (black pluses, Fig. 1). Application of the same linear regression model [(1)] for those conditions results in $m = (2.1 \pm 1.0) \times 10^{-3}$, which is consistent with the m obtained for all observations and supports the hypothesis that surface heat fluxes control N_{tow} by influencing upper-ocean turbulence. Consistent with the forcing imposed in the simulations, we also applied the regression model (1) to observations with $5 < U_{10} < 7 \text{ m s}^{-1}$ and $-200 < I_0 < 500 \text{ W m}^{-2}$ (not shown), resulting in $m = (2.0 \pm 1.2) \times 10^{-3}$, which agrees with the two previous estimates. To investigate the sensitivity of the regression analysis to the nonuniform data distributions, we average the data for $5 < U_{10} < 7 \text{ m s}^{-1}$ into bins using two methods (colored dots in Fig. 1). For the first method (blue dots), we design bins with an equal

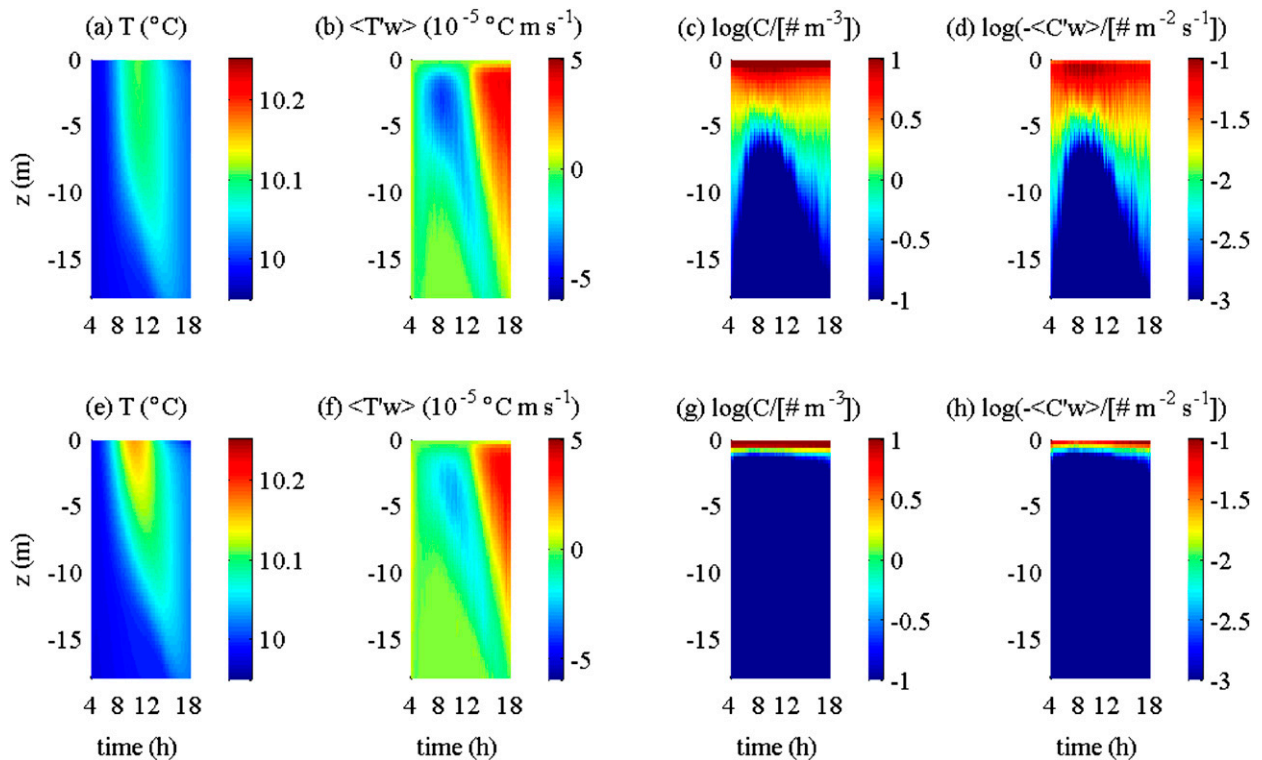


FIG. 2. (a),(e) Simulated evolution of horizontally averaged temperature profiles, (b),(f) resolved turbulent temperature flux, (c),(g) horizontally averaged tracer profiles, and (d),(h) simulated resolved turbulent tracer flux (top) with LT and (bottom) without. Diurnal heating starts at $t = 4$ h, peaks at $t = 8$ h, and stops at $t = 12$ h.

number of points (10% of total number of points in each bin). The second method employs bins with 100 W m^{-2} widths (red dots with number of points in each bin). The regression slope is $m = (2.5 \pm 1.5) \times 10^{-3}$ for the first binning and $m = (2.2 \pm 1.1) \times 10^{-3}$ for the second binning method, indicating that the observed increase of N_{tow} with I_0 is a robust relation in spite of significant scatter. This regression analysis of observations suggests that heating effects can change surface concentrations by more than one order of magnitude from the most extreme cooling to the most extreme heating events. However, it is important to keep in mind potential uncertainties due to errors in I_0 and incomplete knowledge of the statistical distributions of N_{tow} and w_b .

b. Simulations

The OSBL stratifies only weakly with LT (cf. Figs. 2a and 2e) because of the substantially enhanced vertical turbulent temperature fluxes in the presence of LT (cf. Figs. 2b and 2f). This result is qualitatively consistent with the swell study by Kukulka et al. (2013), although LT effects are less pronounced in the current study. With LT the shoaling of the OSBL is delayed and starts during the time of greatest heat fluxes around $t = 8$ h. Although our time-dependent heat flux differs from the constant

heating conditions assumed in most previous LES studies, our results are consistent with previous findings that illustrate the importance of LT in vertical heat transport and the inhibition of diurnal warm layer formation (Li and Garrett 1995; Min and Noh 2004; Noh et al. 2009).

Buoyant tracers are much more deeply submerged with LT than without (cf. Figs. 2c and 2g). Correspondingly, the resolved turbulent tracer fluxes are larger and extend to greater depth (Figs. 2d and 2h). Note that a close relation between tracer concentrations and turbulent tracer fluxes is expected if the buoyant upward transport is balanced by the turbulent downward transport (Kukulka and Brunner 2015). At greater depth, the buoyant tracer profiles remain nearly unchanged without LT during the diurnal heating event. With LT, surface concentration increases and deep submergence decreases during relatively strong surface heating around $t = 8$ h. For $w_b = 1.4 \text{ cm s}^{-1}$, the heating effect is only substantial with LT because convective turbulence and shear-driven turbulence are too weak to submerge plastics below the tow net depth.

With LT, the dependence of N_{tow} on I_0 is more pronounced with changes over the diurnal heat flux cycle of N_{tow} of about 300% and 100% for $w_b = 0.7$ and 1.4 cm s^{-1} , respectively (black symbols, Fig. 3a).

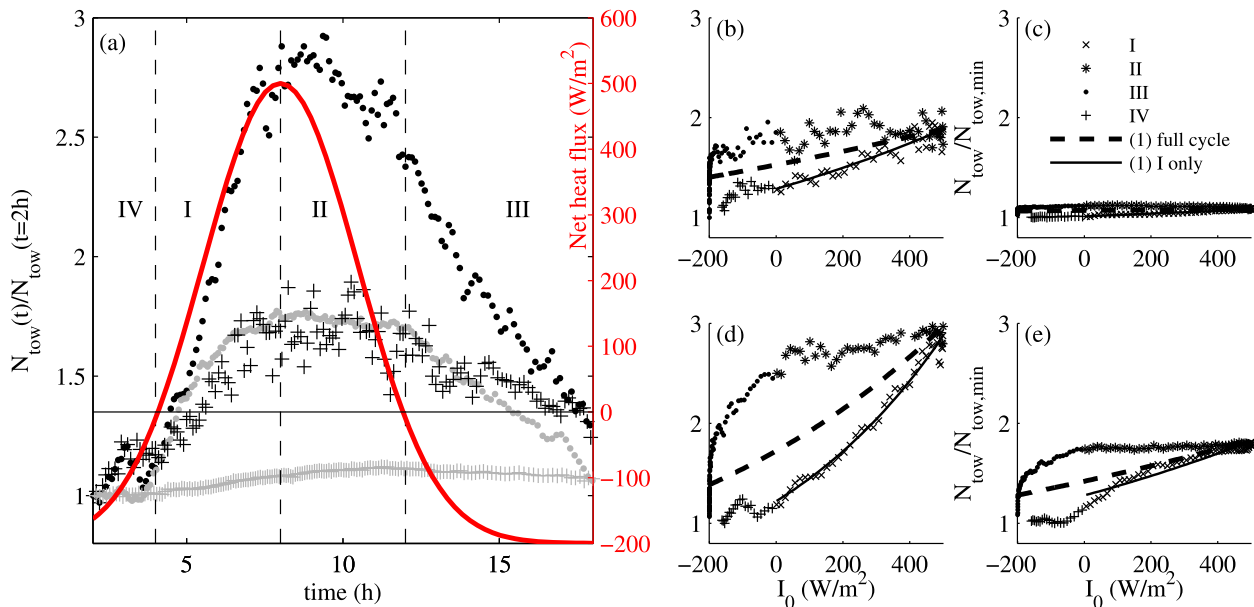


FIG. 3. (a) Modeled surface concentrations of buoyant MPMD (normalized by its value at $t = 2$ h) with (black) and without (gray) LT with $w_b = 0.7 \text{ cm s}^{-1}$ (dots) and $w_b = 1.4 \text{ cm s}^{-1}$ (pluses). The surface heat flux I_0 (red) shows four distinct phases. Hysteresis cycle of N_{tow} normalized by its minimum value as function of I_0 (b),(d) with and (c),(e) without LT for $w_b = 1.4 \text{ cm s}^{-1}$ in (b) and (c) and $w_b = 0.7 \text{ cm s}^{-1}$ in (d) and (e). Different phases of the heating cycle are indicated by corresponding symbols. The regression model [based on (1)] is applied to the full cycle (dashed line) and to phase 1 only (solid line).

Without LT, particles remain surface trapped for $w_b = 1.4 \text{ cm s}^{-1}$ (gray pluses, Fig. 3a). For $w_b = 0.7 \text{ cm s}^{-1}$ and without LT (gray dots, Fig. 3a), variations of N_{tow} are comparable to LT results with $w_b = 1.4 \text{ cm s}^{-1}$ (black pluses, Fig. 3a). Additional LES sensitivity experiments indicate that variations without LT effects are due to the convective mixing that submerges the buoyant tracer sufficiently below the net depth for $w_b = 0.7 \text{ cm s}^{-1}$. However, the buoyant tracer is not as deeply submerged as with LT and $w_b = 1.4 \text{ cm s}^{-1}$ so that the two cases still differ substantially in vertical distributions.

Peak surface concentrations occur between $t = 8$ and 10 h and appear to be delayed relative to the time of maximum surface heating at $t = 8 \text{ h}$ (I_0 is the red line, Fig. 3, left panel). This delay is due to history effects, since heat transport and changes in temperature and turbulence response take time (Noh et al. 2009; Kukulka et al. 2013; Pearson et al. 2015). Model results also suggest that the response to heating is asymmetric so that the response time is faster when the heat flux increases. This hysteresis effect is due to relatively strong turbulence present at the onset of heating, which transports buoyant tracers more efficiently than suppressed turbulence does after prolonged surface heating.

c. Comparison of observations and simulations

Let us first assume that measurements were made during a heat flux cycle that resembles the one from the

idealized LES and compute the same regression slope m in (1) for LES results over the full heat flux cycle (dashed black line Figs. 3b–e). For average $w_b = 1.4 \text{ cm s}^{-1}$, we find $m = (0.42 \pm 0.08) \times 10^{-3}$ with LT and $m = (0.027 \pm 0.018) \times 10^{-3}$ without LT so that only with LT does N_{tow} respond substantially to variations in heat fluxes, consistent with observations (Figs. 3b,c). However, even for the LT solutions, m is smaller than the observed $m = (2.0 \pm 1.2) \times 10^{-3}$ so that the simulated dependence of N_{tow} on I_0 is weaker than observed. For smaller $w_b = 0.7 \text{ cm s}^{-1}$, the regression slope is $m = (1.09 \pm 0.13) \times 10^{-3}$ with LT and $m = (0.51 \pm 0.09) \times 10^{-3}$ without LT (Figs. 3d,e). Thus, the LES experiment with LT and low buoyant rise velocity agrees with the observed $m = (2.0 \pm 1.2) \times 10^{-3}$ if MPMD rise velocities are similar to those in Reisser et al. (2015). Additional empirical measurements of rise velocity are needed to confirm this result.

Our LES results suggest that potential sampling biases for different heating phases due to hysteresis effects need to be taken into account for proper comparisons between the observed and simulated dependence of N_{tow} on I_0 . To examine this, we divide the diurnal heating cycle into four distinct phases: 1) heating increases ($I_0 > 0, \partial I_0 / \partial t > 0$), 2) heating subsides ($I_0 > 0, \partial I_0 / \partial t < 0$), 3) onset of convection ($I_0 < 0, \partial I_0 / \partial t < 0$), and 4) nighttime convection ($I_0 < 0, \partial I_0 / \partial t \geq 0$; Fig. 3). Consistent with the hysteresis effects discussed above,

N_{tow} depends more strongly on I_0 during phases 1 and 3. An analysis of the heat fluxes during the observation period indicates sampling of 36%, 21%, 29%, and 14% in phases 1, 2, 3, and 4, respectively. Therefore, sampling occurs more frequently during phases 1 and 3 so that observed heating effects are likely stronger than expected for the full diurnal cycle. For example, we apply the regression model based on (1) during heating phase 1 to LES results with $w_b = 1.4 \text{ cm s}^{-1}$, which results in $m = (0.76 \pm 0.08) \times 10^{-3}$ with LT and $m = (0.13 \pm 0.09) \times 10^{-3}$ without LT. This result suggests that, for mean w_b , only LT solutions are consistent with observations.

4. Discussion and conclusions

Based on the analysis of observations from the Atlantic and Pacific Oceans and idealized large-eddy simulations (LES), we have provided initial evidence of the influence of ocean surface heat fluxes and Langmuir turbulence (LT) on buoyant microplastic marine debris (MPMD) surface concentrations N_{tow} .

To understand practically the impact of heating during our observation period, we apply (1) for mean wind conditions with $m = 2 \times 10^{-3}$ to find that N_{tow} changes by more than a factor of 2 from its value without surface heat fluxes if $|I_0|$ exceeds about 350 W m^{-2} . During such substantial heating or cooling events, which occur about 10% of the time in our dataset, it is essential to take into account heating effects together with LT in order to accurately interpret surface measurements of buoyant tracer concentrations. Furthermore, sampling strategies for buoyant microplastic debris should be designed to avoid potential biases due to preferential sampling in certain phases of the diurnal heating cycle. In this context, hysteresis effects also need to be considered due to the delayed upper-ocean response to time-dependent surface heating, which were revealed in this study by the LES model. Continuous measurements of surface heat flux prior to and during MPMD sampling would allow this bias to be detected and corrected. Our LES results are more consistent with observations if enhanced mixing due to wave-driven LT is included. Thus, our results demonstrate the controlling influence of combined forcing due to surface heat fluxes, wind, and waves on turbulent transport and vertical distributions of buoyant marine tracers. A more comprehensive analysis requires improved estimates of surface fluxes and wave parameters as well as enhanced estimates of statistical distributions of surface concentrations and buoyant rise velocities.

Acknowledgments. This work was supported by the U.S. National Science Foundation (Grant OCE-1352422). We thank two anonymous reviewers whose constructive

comments have improved the manuscript. We acknowledge computational and staff resources from IT at the University of Delaware. The data for this paper are available from the author Tobias Kukulka (kukulka@udel.edu).

REFERENCES

- Andrady, A., 2011: Microplastics in the marine environment. *Mar. Pollut. Bull.*, **62**, 1596–1605, doi:10.1016/j.marpolbul.2011.05.030.
- Belcher, S. E., and Coauthors, 2012: A global perspective on Langmuir turbulence in the ocean surface boundary layer. *Geophys. Res. Lett.*, **39**, L18605, doi:10.1029/2012GL052932.
- Brunner, K., T. Kukulka, G. Proskurowski, and K. L. Law, 2015: Passive buoyant tracers in the ocean surface boundary layer: 2. Observations and simulations of microplastic marine debris. *J. Geophys. Res. Oceans*, **120**, 7559–7573, doi:10.1002/2015JC010840.
- Colbo, K., and M. Li, 1999: Parameterizing particle dispersion in Langmuir circulation. *J. Geophys. Res.*, **104**, 26 059–26 068, doi:10.1029/1999JC900190.
- Cozar, A., and Coauthors, 2014: Plastic debris in the open ocean. *Proc. Natl. Acad. Sci. USA*, **111**, 10 239–10 244, doi:10.1073/pnas.1314705111.
- D’Asaro, E., 2000: Simple suggestions for including vertical physics in oil spill models. *Spill Sci. Technol. Bull.*, **6**, 209–211, doi:10.1016/S1353-2561(01)00039-1.
- , 2014: Turbulence in the upper-ocean mixed layer. *Annu. Rev. Mar. Sci.*, **6**, 101–115, doi:10.1146/annurev-marine-010213-135138.
- Denman, K. L., and A. E. Gargett, 1995: Biological physical interactions in the upper ocean: The role of vertical and small-scale transport processes. *Annu. Rev. Fluid Mech.*, **27**, 225–256, doi:10.1146/annurev.fl.27.010195.001301.
- Eriksen, M., and Coauthors, 2014: Plastic pollution in the world’s oceans: More than 5 trillion plastic pieces weighing over 250,000 tons afloat at sea. *PLoS One*, **9**, e111913, doi:10.1371/journal.pone.0111913.
- Gargett, A. E., J. Wells, A. E. Tejada-Martinez, and C. E. Grosch, 2004: Langmuir supercells: A mechanism for sediment resuspension and transport in shallow seas. *Science*, **306**, 1925–1928, doi:10.1126/science.1100849.
- Gemmrich, J., 2012: Bubble-induced turbulence suppression in Langmuir circulation. *Geophys. Res. Lett.*, **39**, L10604, doi:10.1029/2012GL051691.
- Gold, M., K. Mika, C. Horowitz, M. Herzog, and L. Leitner, 2013: Stemming the tide of plastic marine litter: A global action agenda. *Pitzker Briefs*, **5**, 1–32.
- Grant, A. L. M., and S. E. Belcher, 2009: Characteristics of Langmuir turbulence in the ocean mixed layer. *J. Phys. Oceanogr.*, **39**, 1871–1887, doi:10.1175/2009JPO4119.1.
- Harcourt, R. R., and E. A. D’Asaro, 2010: Measurement of vertical kinetic energy and vertical velocity skewness in oceanic boundary layers by imperfectly Lagrangian floats. *J. Atmos. Oceanic Technol.*, **27**, 1918–1935, doi:10.1175/2010JTECHO731.1.
- Kalnay, E., and Coauthors, 1996: The NCEP/NCAR 40-Year Reanalysis Project. *Bull. Amer. Meteor. Soc.*, **77**, 437–471, doi:10.1175/1520-0477(1996)077<0437:TNYRP.2.0.CO;2.
- Kukulka, T., and K. Brunner, 2015: Passive buoyant tracers in the ocean surface boundary layer: 1. Influence of equilibrium wind-waves on vertical distributions. *J. Geophys. Res. Oceans*, **120**, 3837–3858, doi:10.1002/2014JC010487.

- , G. Proskurowski, S. Mort-Ferguson, D. W. Meyer, and K. L. Law, 2012: The effect of wind mixing on the vertical distribution of buoyant plastic debris. *Geophys. Res. Lett.*, **39**, L07601, doi:10.1029/2012GL051116.
- , A. J. Plueddemann, and P. P. Sullivan, 2013: Inhibited upper ocean restratification in nonequilibrium swell conditions. *Geophys. Res. Lett.*, **40**, 3672–3676, doi:10.1002/grl.50708.
- Large, W., and S. Pond, 1981: Open ocean momentum flux measurements in moderate to strong winds. *J. Phys. Oceanogr.*, **11**, 324–336, doi:10.1175/1520-0485(1981)011<0324:OOMFMI>2.0.CO;2.
- , J. McWilliams, and S. Doney, 1994: Ocean vertical mixing: A review and a model with a nonlocal boundary layer parameterization. *Rev. Geophys.*, **32**, 363–403, doi:10.1029/94RG01872.
- Law, K. L., S. E. Mort-Ferguson, N. A. Maximenko, G. Proskurowski, E. E. Peacock, J. Hafner, and C. M. Reddy, 2010: Plastic accumulation in the North Atlantic Subtropical Gyre. *Science*, **329**, 1185–1188, doi:10.1126/science.1192321.
- , —, D. S. Goodwin, E. R. Zettler, E. DeForce, T. Kukulka, and G. Proskurowski, 2014: Distribution of surface plastic debris in the eastern Pacific Ocean from an 11-year data set. *Environ. Sci. Technol.*, **48**, 4732–4738, doi:10.1021/es4053076.
- Li, M., and C. Garrett, 1995: Is Langmuir circulation driven by surface waves or surface cooling? *J. Phys. Oceanogr.*, **25**, 64–76, doi:10.1175/1520-0485(1995)025<0064:ILCDBS>2.0.CO;2.
- , K. Zahariev, and C. Garrett, 1995: Role of Langmuir circulation in the deepening of the ocean surface mixed layer. *Science*, **270**, 1955–1957, doi:10.1126/science.270.5244.1955.
- , C. Garrett, and E. Skillingstad, 2005: A regime diagram for classifying turbulent large eddies in the upper ocean. *Deep-Sea Res. I*, **52**, 259–278, doi:10.1016/j.dsr.2004.09.004.
- Liang, J.-H., J. C. McWilliams, P. P. Sullivan, and B. Baschek, 2011: Modeling bubbles and dissolved gases in the ocean. *J. Geophys. Res.*, **116**, C03015, doi:10.1029/2010JC006579.
- McWilliams, J. C., P. P. Sullivan, and C. H. Moeng, 1997: Langmuir turbulence in the ocean. *J. Fluid Mech.*, **334**, 1–30, doi:10.1017/S0022112096004375.
- Min, H. S., and Y. Noh, 2004: Influence of the surface heating on Langmuir circulation. *J. Phys. Oceanogr.*, **34**, 2630–2641, doi:10.1175/JPOJPO-2654.1.
- Noh, Y., G. Goh, S. Raasch, and M. Gryschka, 2009: Formation of a diurnal thermocline in the ocean mixed layer simulated by LES. *J. Phys. Oceanogr.*, **39**, 1244–1257, doi:10.1175/2008JPO4032.1.
- Paulson, C. A., and J. J. Simpson, 1977: Irradiance measurement in the upper ocean. *J. Phys. Oceanogr.*, **7**, 952–956, doi:10.1175/1520-0485(1977)007<0952:IMITUO>2.0.CO;2.
- Pearson, B. C., A. L. M. Grant, J. A. Polton, and S. E. Belcher, 2015: Langmuir turbulence and surface heating in the ocean surface boundary layer. *J. Phys. Oceanogr.*, **45**, 2897–2911, doi:10.1175/JPO-D-15-0018.1.
- Plueddemann, A. J., and R. A. Weller, 1999: Structure and evolution of the oceanic surface boundary layer during the surface waves processes program. *J. Mar. Syst.*, **21**, 85–102, doi:10.1016/S0924-7963(99)00007-X.
- , J. Smith, D. Farmer, R. Weller, W. Crawford, R. Pinkel, S. Vagle, and A. Gnanadesikan, 1996: Structure and variability of Langmuir circulation during the surface waves processes program. *J. Geophys. Res.*, **101**, 3525–3543, doi:10.1029/95JC03282.
- Polton, J. A., and S. E. Belcher, 2007: Langmuir turbulence and deeply penetrating jets in an unstratified mixed layer. *J. Geophys. Res.*, **112**, C09020, doi:10.1029/2007JC004205.
- Price, J., R. Weller, and R. Pinkel, 1986: Diurnal cycling: Observations and models of the upper ocean response to diurnal heating, cooling, and wind mixing. *J. Geophys. Res.*, **91**, 8411–8427, doi:10.1029/JC091iC07p08411.
- Reisser, J., and Coauthors, 2015: The vertical distribution of buoyant plastics at sea: An observational study in the North Atlantic Gyre. *Biogeosciences*, **12**, 1249–1256, doi:10.5194/bg-12-1249-2015.
- Skillingstad, E., 2003: The effects of Langmuir circulation on buoyant particles. *Handbook of Scaling Methods in Aquatic Ecology: Measurement, Analysis, Simulation*, P. G. Strutton and L. Seuront, Eds., CRC Press, 445–457, doi:10.1201/9780203489550.ch28.
- , and D. Denbo, 1995: An ocean large-eddy simulation of Langmuir circulations and convection in the surface mixed layer. *J. Geophys. Res.*, **100**, 8501–8522, doi:10.1029/94JC03202.
- Smith, J. A., 1992: Observed growth of Langmuir circulation. *J. Geophys. Res.*, **97**, 5651–5664, doi:10.1029/91JC03118.
- , 1998: Evolution of Langmuir circulation during a storm. *J. Geophys. Res.*, **103**, 12 649–12 668, doi:10.1029/97JC03611.
- Soloviev, A., and R. Lukas, 1997: Observation of large diurnal warming events in the near-surface layer of the western equatorial pacific warm pool. *Deep-Sea Res. I*, **44**, 1055–1076, doi:10.1016/S0967-0637(96)00124-0.
- Sullivan, P. P., and J. C. McWilliams, 2010: Dynamics of winds and currents coupled to surface waves. *Annu. Rev. Fluid Mech.*, **42**, 19–42, doi:10.1146/annurev-fluid-121108-145541.
- Tejada-Martinez, A. E., and C. E. Grosch, 2007: Langmuir turbulence in shallow water. Part 2. Large-eddy simulation. *J. Fluid Mech.*, **576**, 63–108, doi:10.1017/S0022112006004587.
- Thorpe, S. A., 1982: On the clouds of bubbles formed by breaking wind-waves in deep water, and their role in air–sea gas transfer. *Philos. Trans. Roy. Soc. London*, **A304**, 155–210, doi:10.1098/rsta.1982.0011.
- , 2004: Langmuir circulation. *Annu. Rev. Fluid Mech.*, **36**, 55–79, doi:10.1146/annurev.fluid.36.052203.071431.
- Weller, R. A., and J. F. Price, 1988: Langmuir circulation within the oceanic mixed layer. *Deep-Sea Res.*, **35A**, 711–747, doi:10.1016/0198-0149(88)90027-1.
- Wyngaard, J. C., 2010: *Turbulence in the Atmosphere*. 1st ed. Cambridge University Press, 393 pp.
- Yang, D., M. Chamecki, and C. Meneveau, 2014: Inhibition of oil plume dilution in Langmuir ocean circulation. *Geophys. Res. Lett.*, **41**, 1632–1638, doi:10.1002/2014GL059284.